Available online at www.sciencedirect.com
ScienceDirect
Biomaterials 29 (2008) 2464–2476
Biomaterials
www.elsevier.com/locate/biomaterials

Introduction of enzymatically degradable poly(trimethylene carbonate) microspheres into an injectable calcium phosphate cement

Wouter J.E.M. Habraken [a], Zheng Zhang [b], Joop G.C. Wolke [a], Dirk W. Grijpma [b,c], Antonios G. Mikos [d], Jan Feijen [b], John A. Jansen [a,*]

[a] Department of Periodontology and Biomaterials, College of Dental Science, Radboud University, Nijmegen Medical Center, Nijmegen, The Netherlands
[b] Institute for Biomedical Technology (BMTI) and Department of Polymer Chemistry and Biomaterials, Faculty of Science and Technology, University of Twente, Enschede, The Netherlands
[c] Department of Biomedical Engineering, University Medical Center Groningen, University of Groningen, Groningen, The Netherlands
[d] Department of Bioengineering, Rice University, Houston, Texas, USA

Received 21 December 2007; accepted 13 February 2008
Available online 6 March 2008

Abstract

Poly(trimethylene carbonate) (PTMC) is an enzymatically degradable polyester with rubber-like properties. Introduction of this polymer into an injectable calcium phosphate bone cement can therefore be used to introduce macroporosity into the cement for tissue engineering purposes as well as to improve mechanical properties. Aim of this study was to investigate calcium phosphate cements with incorporated PTMC microspheres (PTMC CPCs) on their physical/mechanical properties and *in vitro* degradation characteristics. Therefore, composites were tested on setting time and mechanical strength as well as subjected to phosphate buffered saline (PBS) and enzyme containing medium. PTMC CPCs (12.5 and 25 wt%) with molecular weights of 52.7 kg mol^{-1} and 176.2 kg mol^{-1} were prepared, which showed initial setting times similar to that of original CPC. Though compression strength decreased upon incorporation of PTMC microspheres, elastic properties were improved as strain-at-yield increased with increasing content of microspheres. Sustained degradation of the microspheres inside PTMC CPC occurred when incubated in the enzymatic environment, but not in PBS, which resulted in an interconnected macroporosity for the 25 wt% composites.

Keywords: Calcium phosphate cement; Poly(trimethylene carbonate); Microspheres; Degradation; Mechanical strength

1. Introduction

Calcium phosphate cements are used in clinical practice for filling up bone defects because of their biocompatibility, osteoconductivity and perfect fit with the surrounding tissue when injected *in situ* [1]. For bone tissue engineering purposes, resorption of dense cement is too slow [2]. Therefore, (macro)porosity is often introduced to enable bone ingrowth into the material concomitantly improving the bioresorption [3]. Incorporation of poly(lactic-*co*-glycolic) acid (PLGA) or gelatin microspheres in calcium phosphate cements [4–6] has proven to introduce macroporosity during *in situ* degradation of the microspheres without unacceptably affecting the handling properties or cement setting. A rationale for this construct is that bone ingrowth compensates for the loss of mechanical strength, which occurs as a result of microsphere degradation. Furthermore, these microspheres can be used as drug delivery vesicles for osteoinductive growth factors [7,8], thereby improving the often marginal release from these cements.

Despite the favorable release of growth factors we observed also that inclusion of PLGA microspheres was associated with a loss of mechanical strength of the set cement as well as the production of acidic degradation products [4]. The subsequent

* Corresponding author. Department of Periodontology and Biomaterials, College of Dental Science, Radboud University Nijmegen Medical Centre, P.O. Box 9101, 6500 HB Nijmegen, The Netherlands. Tel.: +31 24 3614006; fax: +31 24 3614657.
E-mail address: j.jansen@dent.umcn.nl (J.A. Jansen).

0142-9612/$ - see front matter © 2008 Elsevier Ltd. All rights reserved.
doi:10.1016/j.biomaterials.2008.02.012

replacement of PLGA with gelatin microspheres resulted in a more gradual degradation, which occurred from the outer to the inner part of the cement composite, where degradation was dependent on the type and amount of incorporated microspheres [5,6]. Unfortunately, the gelatin degrading enzyme (collagenase) experienced physical interactions with the surrounding calcium phosphate cement, delaying degradation of microspheres at the inner parts. Another setback is that gelatin exhibits biomimetic properties [9]. As a consequence, the microspheres became often completely covered by a calcium phosphate precipitate that decreased the interconnectivity of the spheres and thereby also penetration of the enzyme.

Poly(trimethylene carbonate) (PTMC, Fig. 1) is a flexible, biodegradable polymer that in contrast to PLA/PLGA does not produce acidic degradation products [10]. PTMC degrades via surface erosion, i.e. degradation occurs only at the surface resulting in a decrease of size/radius of the material [11]. Studies have shown that this process is driven by enzymatic degradation where degradation rates can be increased by increasing the molecular weight of the polymer [11,12]. It can be hypothesized that upon introduction of PTMC microspheres [13] into an injectable calcium phosphate cement a controlled degradation pattern will occur without the problems as observed with gelatin. Furthermore, the rubber-like properties of PTMC can possibly also be used to improve the initial mechanical properties of the cement.

In view of the above mentioned, the goal of this study was to formulate a PTMC microsphere/calcium phosphate cement composite (PTMC CPC) with appropriate handling properties and to investigate the mechanical properties and *in vitro* degradation characteristics. Therefore, the 12.5 and 25 wt% PTMC CPCs were prepared using PTMC with molecular weights of 52.7 kg mol^{-1} and 176.2 kg mol^{-1}. Setting time, porosity and mechanical characteristics of the different formulations were determined. For the *in vitro* degradation assay, samples were subjected to enzyme containing medium (lipase) or phosphate buffered saline (PBS). The pH of the medium was monitored and samples were assayed on mass loss, compression strength, E-modulus, chemical consistency (FTIR, XRD) and morphology (SEM).

2. Materials and methods

2.1. Materials

$PTMC_{53}$ ($M_n = 52.7$ kg mol^{-1}, $M_w = 84.1$ kg mol^{-1}, PDI = 1.60) and $PTMC_{176}$ ($M_n = 176.2$ kg mol^{-1}, $M_w = 265.2$ kg mol^{-1}, PDI = 1.51) were synthesized by ring opening polymerization [13] and used for the preparation of the microspheres. The applied CaP cement is commercially available under the product name Calcibon® and consists of 61 wt% α-TCP, 26 wt% $CaHPO_4$, 10 wt% $CaCO_3$ and 3 wt% pHA. Lipase from *Thermomyces lanuginosus* (EC 3.1.1.3, minimum 100 000 units/g, Sigma–Aldrich, St. Louis, USA) was used as PTMC degrading enzyme solution.

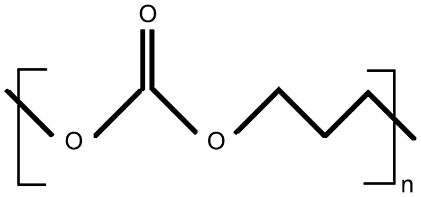

Fig. 1. Chemical structure of poly(trimethylene carbonate).

2.2. Preparation of PTMC microspheres

PTMC microspheres were prepared by a single emulsion method. Briefly, 1 wt% of $PTMC_{176}$ and 2 wt% of $PTMC_{53}$ solution in dichloromethane was emulsified in an aqueous phase containing 2% PVA. The stirring speeds were, respectively, 1000 rpm and 800 rpm. After evaporation of dichloromethane, microparticles were solidified, and then purified by centrifugation and re-dispersed in the PVA-containing aqueous phase.

Morphology of the $PTMC_{53}$ and $PTMC_{176}$ microspheres was determined by scanning electron microscopy (SEM, JEOL 6400-LINK AN 10 000 at 10 kV); samples were dried on carbon tape and sputtered with gold–palladium prior to measurement. In addition, morphology of the microspheres was also visualized by light microscopy (Leica Microsystems AG, Wetzlar, GER) after which particle size distributions were determined using digital image software (Leica Qwin, Leica).

2.3. Preparation of PTMC CPC

PTMC microsphere/calcium phosphate cements (PTMC CPCs, 12.5 and 25 wt%) of both $PTMC_{53}$ and $PTMC_{176}$ polymers were prepared. For this, the amount of PTMC microspheres inside the suspension was pooled and microsphere suspensions containing 125/250 mg of microspheres were centrifuged and decanted. Then, 290/260 μl of 1% Na_2HPO_4 was added to the microspheres and the resulting suspension was added to 875/750 mg of CPC inside a 2 ml syringe and stirred vigorously for 15 s using a Silamat® mixing device (Vivadent, Schaan, Liechtenstein). Cement paste was injected into a Teflon mould (cylinders 4.5 × 9.0 mm) and samples were left to set at room temperature over night. The applied concentration and amount of liquid hardener for both the 12.5 and 25 wt% PTMC CPCs were sufficient to accomplish a fully injectable calcium phosphate cement [4]. After drying, cross-sections of the composites were made and the morphology was determined by SEM.

2.4. Setting time

Initial and final setting times were assessed using custom available Gillmore needles (ASTM C266). Therefore, a bronze block containing 6 holes (6 mm in diameter, 12 mm in height) was used as a mould and placed in a water bath at body temperature (37 °C). Samples were mixed and injected into the mould in a retrograde fashion, after which the initial and final setting times were determined [4]. Tests were done in triplicate.

2.5. Porosity

The macro- and total porosity of preset samples was determined. Macroporosity is the porosity generated by the PTMC microspheres and corresponds to the vol% of microspheres. The total porosity is the macroporosity plus the original microporosity of the cement.

To measure these parameters, both PTMC CPC samples and CPC samples of a known volume were placed in an oven at 650 °C for 2 h. After burning out the PTMC or moisture, samples were weighed and Eqs. (1) and (2) were used for the derivation of the total porosity and the macroporosity.

$$\varepsilon_{tot} = \left(1 - \frac{m}{V \times \rho_{HAP}}\right) \times 100\% \quad (1)$$

$$\varepsilon_{macro} = \left(1 - \frac{m_{macro}}{m_{micro}}\right) \times 100\% \quad (2)$$

where ε_{tot} = total porosity (%), ε_{macro} = macroporosity (%), m = average mass sample (g, $n = 3$), m_{macro} = average mass macroporous sample (after burning

out PTMC) (g, $n = 3$), m_{micro} = average mass microporous sample (CPC) (g, $n = 3$), V = volume sample (cm^3), ρ_{HAP} = density hydroxy apatite (g/cm^3).

2.6. Mechanical characteristics

Preset PTMC CPC samples (cylinders, 4.5 mm diameter × 9.0 mm height) were soaked in PBS for 3 days. Subsequently, samples were dried over night in a freeze-dryer, placed in a testing bench (858 MiniBionixII®, MTS Corp., Eden Prairie, MN, USA) and compression strength, E-modulus and strain-at yield (ε) along the vertical axis (height) of the specimens were measured at 0.5 mm/min crosshead speed.

2.7. Degradation assay

For the degradation assay, preset 12.5/25 wt% $PTMC_{53}$ CPC and $PTMC_{176}$ CPC samples were put in 3 ml of a 1:2 lipase/demineralized water solution or PBS (pH = 7.4) for a total of 6 and 12 weeks, respectively. Sample medium was refreshed every week. At days 3, 7, 14, 28, 42 and 84, five samples of each formulation were subjected to analysis as summarized below. CPC samples were taken as reference.

2.7.1. pH measurement

Corresponding to an earlier performed study using PLGA microsphere/calcium phosphate cement composites [4], the pH of the PBS medium was monitored to observe whether conditioning in PBS leads to the formation of acidic compounds.

2.7.2. Mass loss

Sample weight was measured after removal from the incubation medium and freeze-drying over night. Mass loss with time (days) was determined using Eq. (3).

$$R_L = \frac{m_0 - m_n}{m_0} \times 100\% \quad (3)$$

where R_L = mass loss of the sample (%) on $t = n$, m_0 = mass of the sample (g) on $t = 0$, m_n = mass of the sample (g) when $t = n$.

2.7.3. Mechanical characteristics

Compression strength and E-modulus of dried samples were determined by placing the samples in a testing bench as described earlier.

2.7.4. IR spectroscopy

A fraction of the PTMC CPCs samples was grinded and measured by attenuated reflectance Fourier transform infrared spectroscopy (ATR-FTIR, Perkin–Elmer, Fremont, CA, USA). Concentration of PTMC inside the samples was determined analogous to Featherstone et al. [14]. In brief, the extinction of a typical PTMC absorption band (C═O, 1750 cm^{-1}) and a calcium phosphate absorption band (PO_4, 1050 cm^{-1}) of the PTMC CPC was determined using Eq. (4). The resulting ratio of both extinctions ($E_{C=O}/E_{PO4}$) is linear with the percentage of PTMC inside the cement. Therefore, composites with different contents of PTMC CPC (5, 10, 15, 20, 25 and 30 wt%) were prepared and used to make a standard curve.

$$E = \log \frac{T_{baseline}}{T_{sample\text{-}peak}} \quad (4)$$

where E = extinction, $T_{baseline}$ = transmission baseline, $T_{sample\text{-}peak}$ = transmission sample peak.

2.7.5. Thermogravimetric analysis

Samples for the FTIR standard curve were calibrated using thermogravimetric analysis (TGA 7, Perkin–Elmer). For this assay, 30 mg of sample was placed in the instrument where it was kept at 50 °C for 2 min before scanning it from 50 °C to 650 °C at a rate of 10 °C per min. Finally, the sample was kept at 650 °C for 2 min before it was cooled down.

2.7.6. X-ray diffraction spectroscopy

The composition of the cement inside the composites was determined by powder X-ray diffraction (XRD, Philips, PW 3710, Almelo, The Netherlands). Therefore, the same grinded samples were used as for FTIR.

2.7.7. Morphology

Cross-sections of the samples were prepared, morphology of the cement and microspheres at the surface and inner part of the composite were monitored at different magnifications by SEM.

2.8. Statistical analysis

Data were arranged as mean ± standard deviation. Significant differences were determined using analysis of variance (ANOVA). Results were considered significant if $p < 0.05$. Calculations were performed using GraphPad Instat® (GraphPad Software Inc., San Diego, Ca, USA).

3. Results

3.1. Preparation of PTMC microspheres

Investigation by SEM and light microscopy revealed that microspheres of both $PTMC_{53}$ and $PTMC_{176}$ polymers showed a spherical structure with a smooth surface. Average size of the microspheres was higher for the $PTMC_{53}$ polymer (28.6 μm, Table 1) compared to the $PTMC_{176}$ polymer (15.3 μm). $PTMC_{176}$ microspheres showed a narrow particle size distribution with a maximum particle size <40 μm, whereas $PTMC_{53}$ microspheres showed a much broader particle size distribution with a maximum size up to 90 μm.

3.2. Preparation/mechanical properties of PTMC CPC

Fig. 2 shows SEM micrographs of the as-prepared 25 wt% $PTMC_{53}$ CPC and after burning out of the microspheres for the porosity measurements. From the left picture, it could be observed that spheres inside the cement were present with a thin layer of calcium phosphate precipitate onto the surface. The right picture shows that the pores formed by the microspheres are spherical and have a homogenous distribution inside the cement.

Results of the setting time, porosity measurements and mechanical characteristics of the composites are shown in Table 1. Initial setting time of both PTMC CPC composites was similar to the original CPC, whereas final setting time was significantly increased with the 12.5 wt% PTMC CPC and the 25 wt% PTMC CPC. Porosity measurements showed a total porosity of ±60% and 70% with the 12.5 and 25 wt% PTMC CPC, respectively, while the microporosity of the original cement reached values up to 40%. Calculated macroporosity (% spheres inside the cement) increased with increasing amount of microspheres, and reached 49% with both the 25 wt% PTMC CPCs. For the 12.5 wt% PTMC CPC samples, macroporosity differed significantly ($p < 0.05$) between both $PTMC_{53}$ and $PTMC_{176}$ composites. Compression strength and E-modulus of the PTMC CPCs were significantly lower compared with CPC and decreased with increasing amount of microspheres ($p < 0.05$). The E-modulus was dependent on the molecular weight of the

Table 1
Physical/mechanical properties PTMC CPCs and CPC

Formulation	CPC	$PTMC_{53}$ CPC		$PTMC_{176}$ CPC	
Average size microspheres (μm)	–	28.63 ± 16.70		15.30 ± 6.21	
PTMC microspheres (wt%)	*0%*	*12.5%*	*25%*	*12.5%*	*25%*
Mass samples (mg)	262.7 ± 6.1	200.0 ± 6.3	178.9 ± 6.7	198.1 ± 6.7	177.5 ± 6.7
Initial setting time (s)	108.3 ± 5.8	105.0 ± 0.0	183.3 ± 31.8	110.0 ± 8.7	170.0 ± 34.6
Final setting time (s)	235.0 ± 31.2	480.0 ± 17.3	>1200[a]	480.0 ± 42.4	>1200[a]
Total porosity (%)	40.8 ± 1.3	57.3 ± 0.5	69.6 ± 0.6	62.5 ± 1.5	70.0 ± 0.4
Macroporosity (%)	0	27.9 ± 1.4	48.7 ± 1.4	36.7 ± 1.9	49.3 ± 1.3
Compression strength (MPa, $n = 7$)	64.4 ± 16.6	19.0 ± 3.1	15.5 ± 2.6	23.9 ± 4.8	15.3 ± 1.6
E-modulus (GPa, $n = 7$)	5.44 ± 1.33	1.14 ± 0.23	0.68 ± 0.13	1.60 ± 0.62	1.13 ± 0.27
Strain-at-yield (ε, mm, $n = 7$)	0.186 ± 0.011	0.299 ± 0.034	0.386 ± 0.116	0.215 ± 0.021	0.271 ± 0.071

[a] Experiment stopped after 20 min, the specimens hardened within 1 day.

PTMC used for the microspheres as significant higher values were observed for $PTMC_{176}$ CPC as compared to $PTMC_{53}$ CPC. Strain-at-yield (ε) of the PTMC CPC samples increased with increasing amount of PTMC microspheres and was significantly higher ($p < 0.05$) than that of CPC. Also, for $PTMC_{53}$ CPCs a higher ε was observed ($p < 0.05$) than $PTMC_{176}$ CPCs. Furthermore, under high compression PTMC CPC did not fracture into separate smaller pieces but was kept together by the elongated microspheres as depicted in Fig. 3A. From stress–strain curves of compression strength measurements (Fig. 3B), the same phenomenon was observed with especially the 25 wt% PTMC CPC as compression strength remained at a constant level after reaching yield strengths.

3.3. Degradation in PBS

Results for the degradation of PTMC CPC in PBS are given in Figs. 4–7. Release of acidic products from the CPC into the medium (Fig. 4A) resulted in a pH of 6.6 after 21–42 days. Thereafter, the pH decrease was less and the pH slowly returned to its original value after 84 days. The PTMC CPC formulations showed a pattern similar to CPC, but exhibited an overall smaller decrease in pH. For the 25 wt% PTMC CPCs, also a faster increase in pH after 14–28 days was observed. The mass change of the samples with time (Fig. 4B) showed an initial increase in mass of 1.5–3.0% for all samples after 3 days incubation time, after which the mass slowly decreased with time. Though changes in mass were small, significant differences ($p < 0.05$) between the formulations were observed and the initial mass increase was in the following order: CPC > 12.5 wt% PTMC CPC > 25 wt% PTMC CPC. Compression strength and E-modulus of the PTMC CPC and CPC samples (Fig. 4C and D) were constant over time, but, at $t = 14$ and 28 days values with the 12.5 wt% $PTMC_{53}$ CPC were slightly higher. Furthermore, compression strength of the 25 wt% PTMC CPCs showed a significant decrease after 84 days ($p < 0.005$). SEM micrographs of the PTMC CPC composites (Fig. 5) show spherical pores and microsphere structures that are scattered evenly throughout the cement. For the 12.5 wt% PTMC CPC, these pores/spheres are isolated inside the cement, whereas for the 25 wt% PTMC CPC there is a tight packing. However, interconnections between pores are very scarce. Due to the different microsphere sizes, there is a slight difference in pore size between the $PTMC_{53}$ CPC and $PTMC_{176}$ CPC. No clear differences in morphology were observed between samples taken at $t = 42$ days and other time points (data not shown). FTIR was performed to

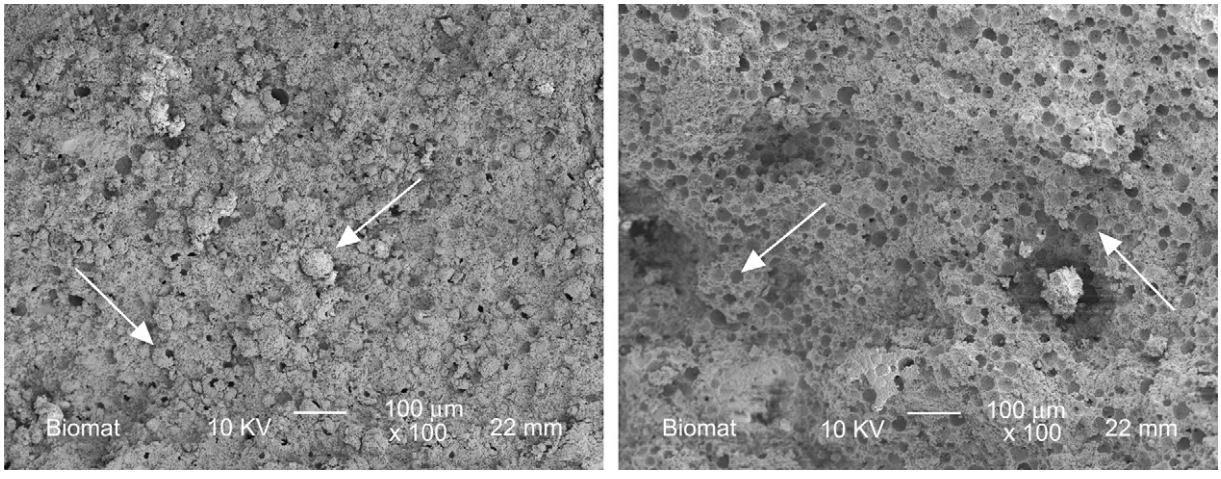

Fig. 2. Morphology of the 25 wt% $PTMC_{53}$ CPC as-prepared (left) and after burning out polymer (right), arrows indicate microspheres or pores (original magnification 100×).

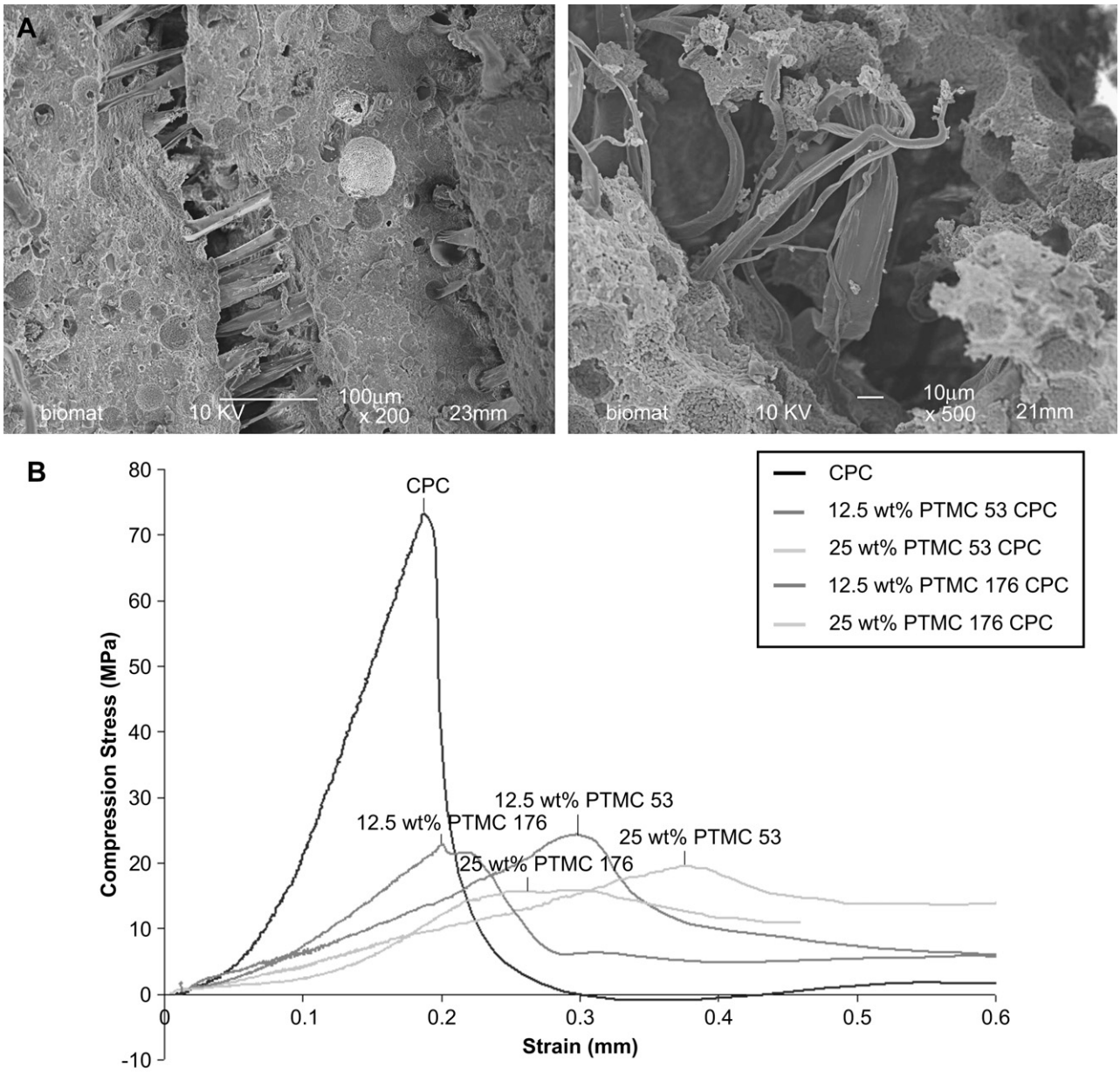

Fig. 3. (A). Stretching of PTMC microspheres at fracture interface (original magnification 200× (left) and 500× (right)); (B) stress–strain curves of CPC and the 12.5/25 wt% PTMC CPCs.

quantitatively determine the amount of PTMC inside the composites. Standard curves that were analyzed with FTIR (and calibrated with TGA) showed a linear relationship between the $E_{C=O}/E_{PO4}$ ratio and PTMC content ($r^2 > 0.98$) for both $PTMC_{53}$ and $PTMC_{176}$ polymers. Using these standard curves, the percentage of PTMC inside the composites was calculated as is shown in Fig. 6. In PBS, both $PTMC_{53}$ and $PTMC_{176}$ CPCs showed a similar trend and a slight increase in %PTMC over time with the 25 wt% PTMC CPCs was determined, whereas the 12.5 wt% PTMC CPCs showed a slight decrease of PTMC content after 84 days. Investigation of the cement structure of the PTMC CPCs by X-ray diffraction (Fig. 7, PBS) revealed that the cement starting compounds (α-TCP, monetite) disappeared within 14 days of incubation, with only the endproduct (apatite) remaining.

3.4. Degradation in lipase solution

Results of the degradation of PTMC CPC in lipase solution are depicted in Figs. 7–11. Mass change of the PTMC CPCs with time (Fig. 8A) showed different curves for both the 12.5 and 25 wt% PTMC CPCs. For the 12.5 wt% PTMC CPC, there was an initial increase in mass of 2% after 3 days that significantly increased to 3.5% after 42 days ($p < 0.005$). The 25 wt% PTMC CPC samples showed a decrease in mass with 1.1–1.7 wt% after 7 days after which also a slight

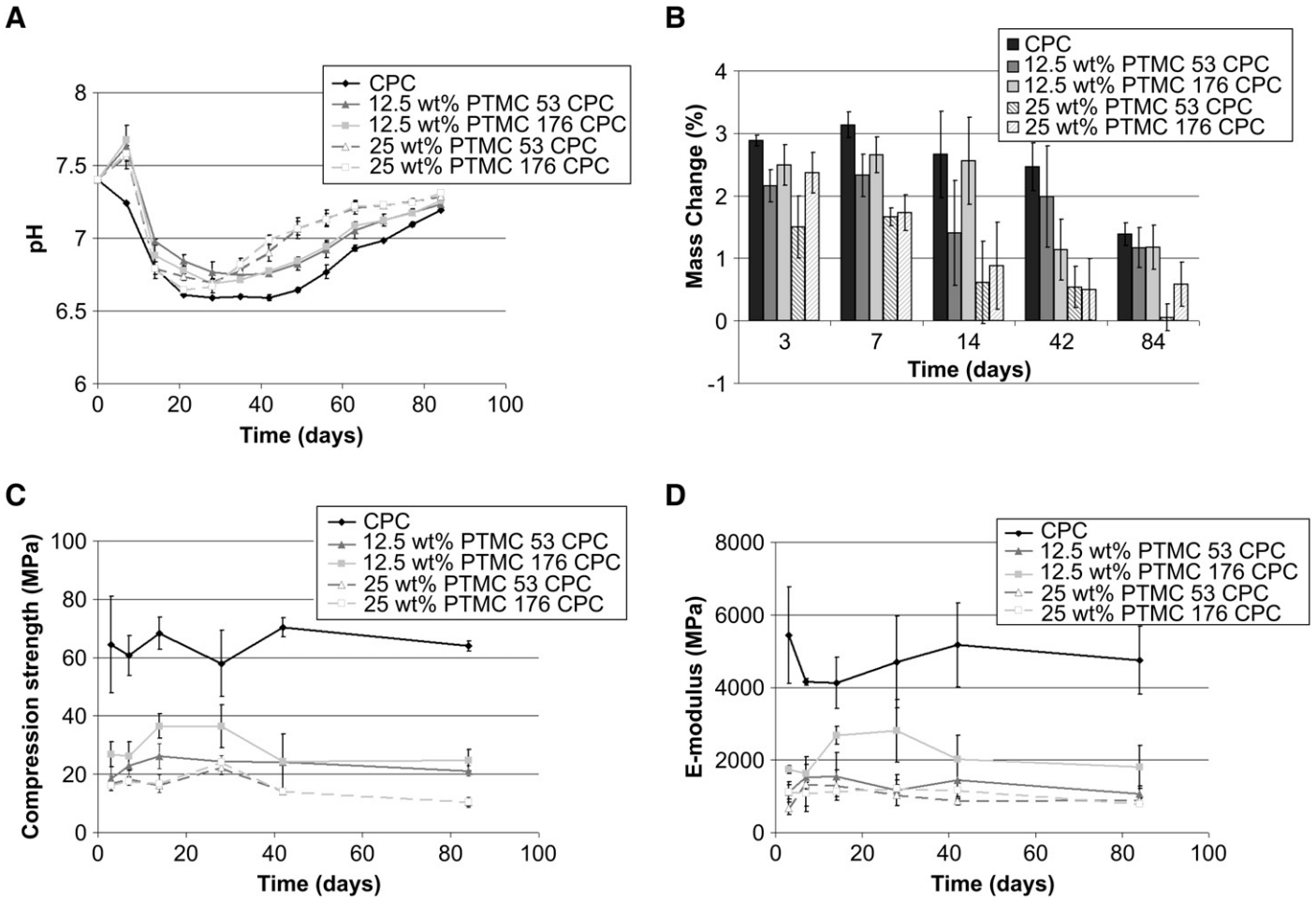

Fig. 4. Degradation of PTMC CPC in PBS: (A) pH change of medium per week; (B) Mass change with time; (C) compression strength with time; (D) E-modulus with time.

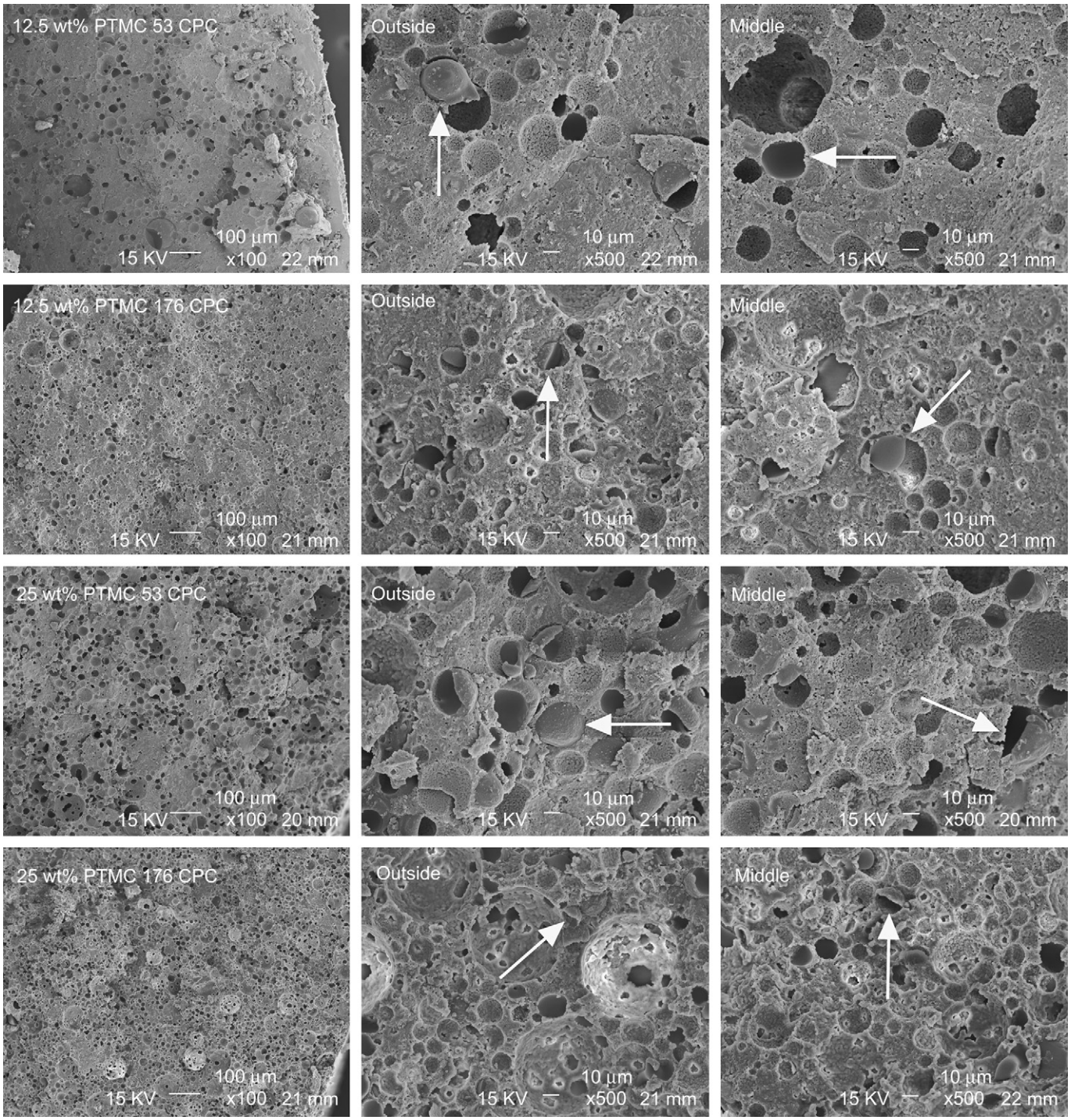

Fig. 5. SEM micrographs of the 12.5 and 25 wt% $PTMC_{53}$ CPC/$PTMC_{176}$ CPC samples after 42 days in PBS, arrows denote PTMC microspheres/shells (original magnification 100× and 500×).

increase in mass was observed. Compression strength (Fig. 8B) of the 25 wt% PTMC CPC (5–10 MPa) at most time points was significantly lower than that for the 12.5 wt% PTMC CPC (15–22 MPa) and did not show a clear trend with time. The E-modulus of both systems (data not shown) showed a similar trend as the compression strength, though less significant differences were observed. SEM micrographs of the 25 wt% PTMC CPCs (Fig. 9) at day 3 show an open porous structure at the outside of the samples, whereas in the inside microspheres were present. A similar morphology was observed after 42 days, though the amount of microspheres present in the middle was markedly reduced. Conversely, with the 12.5 wt% PTMC CPC (Fig. 10) a lot of microspheres were visible at $t = 3$ and 42 days and only at the upper 200 µm of the samples the amount of microspheres was reduced. Furthermore, the cement microstructure of

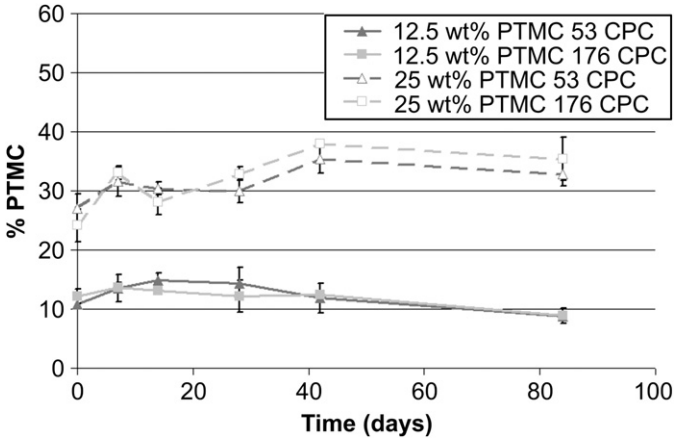

Fig. 6. Weight% of PTMC in samples as measured by FTIR as function of incubation time in PBS.

especially the 25 wt% PTMC CPCs showed a strikingly high porosity. Results from FTIR spectroscopy are given in Fig. 11A and B. Fig. 11A gives a representation of the acquired IR spectra with the 25 wt% $PTMC_{53}$ CPC after $t = 7$, 14, 28 and 42 days. A distinct decrease of peak intensity of all separate PTMC peaks was observed with increasing degradation times, whereas the PO_4-peak of the CaP cement remained constant. Furthermore, a peak at 1650 cm^{-1} was present that was absent for PTMC CPC in PBS medium, showing a slight increase with time. As this wavelength corresponds to the C═O stretch of proteins/amides, this peak may indicate the presence of lipase inside the scaffolds. Fig. 11B shows the wt% of PTMC inside the composite as a function of degradation time. For both the 25 wt% PTMC CPC samples, a significant decrease in the wt% of PTMC was observed from the 25 wt% to 5–8 wt% at 42 days that was faster with the $PTMC_{53}$ CPC. The composition of the 12.5 wt% PTMC CPCs did vary less with time, although also a small decrease in the wt% of PTMC was noted. Finally, the analysis of the cement by XRD (Fig. 7, lipase) revealed that after 14 days of incubation peaks of monetite and α-TCP were still present, though, also here, cement was converted into apatite.

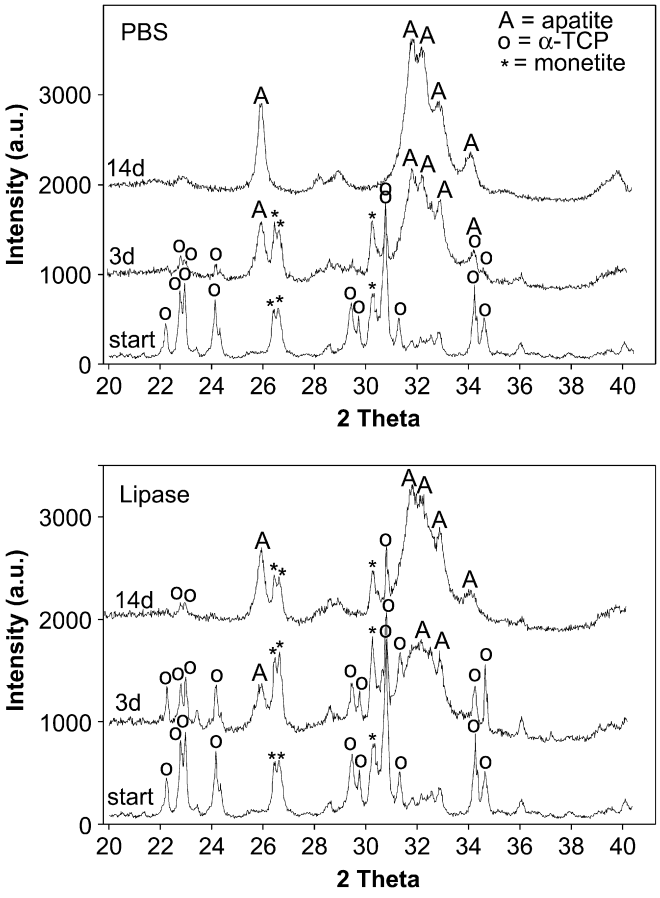

Fig. 7. XRD spectra of cement, starting material and the 25 wt% $PTMC_{53}$ CPC after 3 and 14 days in PBS and lipase solution; figure legend: A = apatite, o = α–TCP, * = monetite.

4. Discussion

In this study, physical/mechanical properties and *in vitro* degradation characteristics of injectable calcium phosphate cement with incorporated PTMC microspheres were investigated. Therefore, the 12.5 and 25 wt% $PTMC_{53}$ and $PTMC_{176}$ microsphere/calcium phosphate cement composites

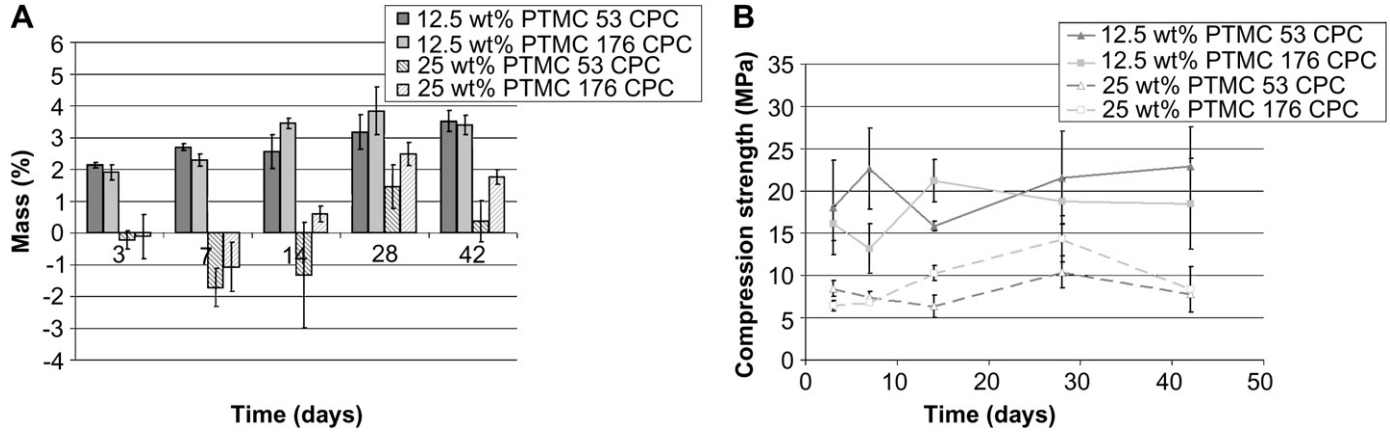

Fig. 8. Degradation of PTMC CPC in lipase solution: (A) mass change with time; (B) compression strength with time.

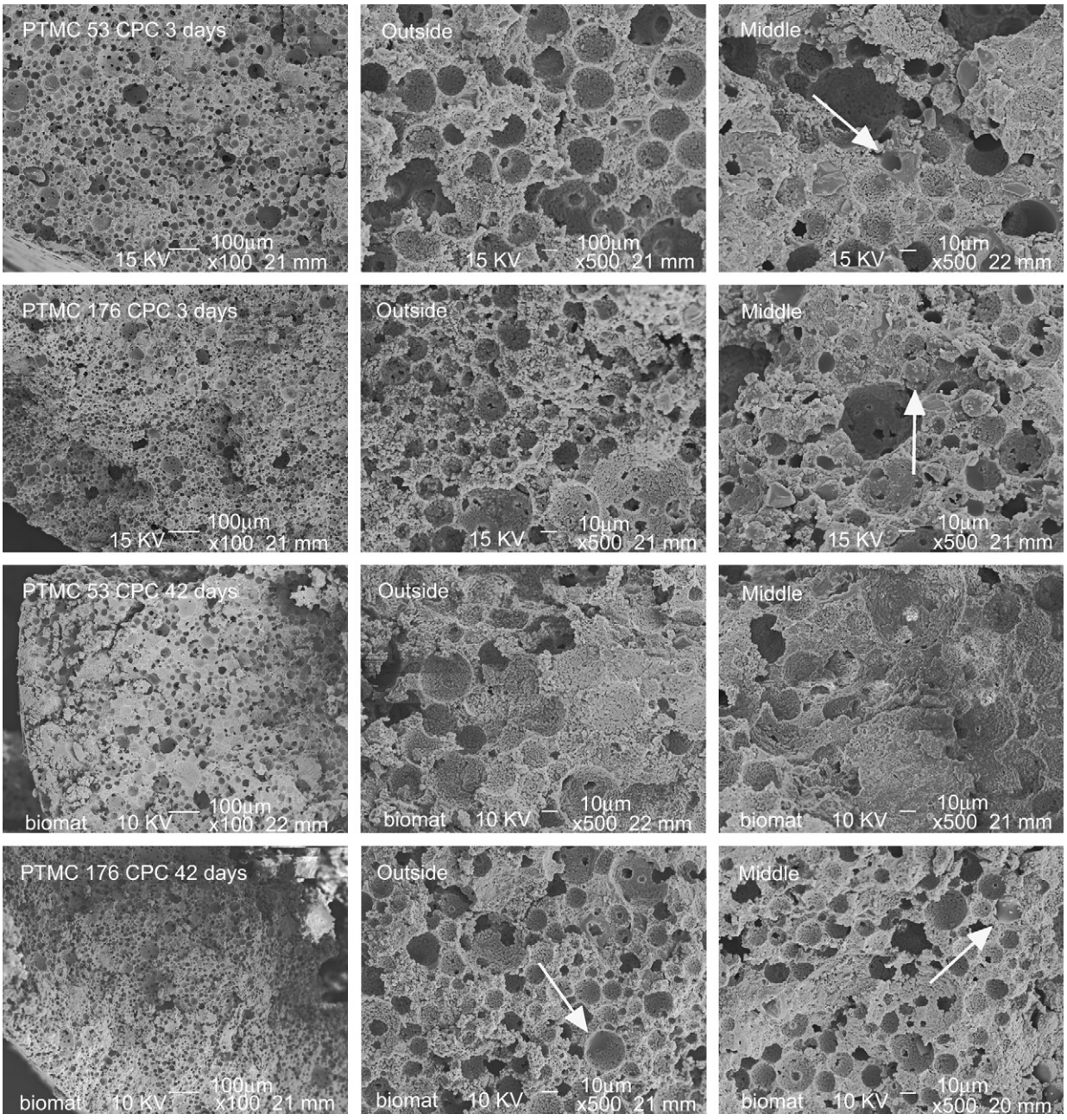

Fig. 9. SEM micrographs of the 25 wt% $PTMC_{53}$ CPC and $PTMC_{176}$ CPC samples after 3 and 42 days in lipase solution, arrows denote PTMC microspheres/shells (original magnification 100× and 500×).

were formulated, which were tested on setting properties, mechanical strength and macroporosity. Furthermore, preset samples were incubated in PBS/lipase and assayed for weight loss, mechanical strength, morphology and composition (XRD, FTIR).

The used poly(trimethylene carbonate) is a polymer with a glass transition temperature (T_g) ~−20°C [15]. Consequently, at room and body temperature PTMC behaves as a rubber-like polymer. During preparation of polymeric microsphere CPC composites, (freeze-)dried microspheres are usually mixed with calcium phosphate cement powder to obtain a good distribution of the microspheres, after which liquid hardener is added [4]. Due to its low T_g, freeze-dried PTMC microspheres agglomerate and therefore cannot be mixed with the cement powder. Therefore, to obtain a PTMC CPC, microspheres were added to the liquid hardener during cement preparation as described in Section 2, which resulted in a well distributed microsphere composite. In agreement with previous studies using PLGA and gelatin microspheres [4,5], setting time was increased upon addition of the PTMC microspheres. When compared to conventional CPC [16] setting time increased due to an increase in liquid/powder ratio as extra aqueous phase was still present after carefully decanting the PVA solution above the PTMC microspheres. Also with

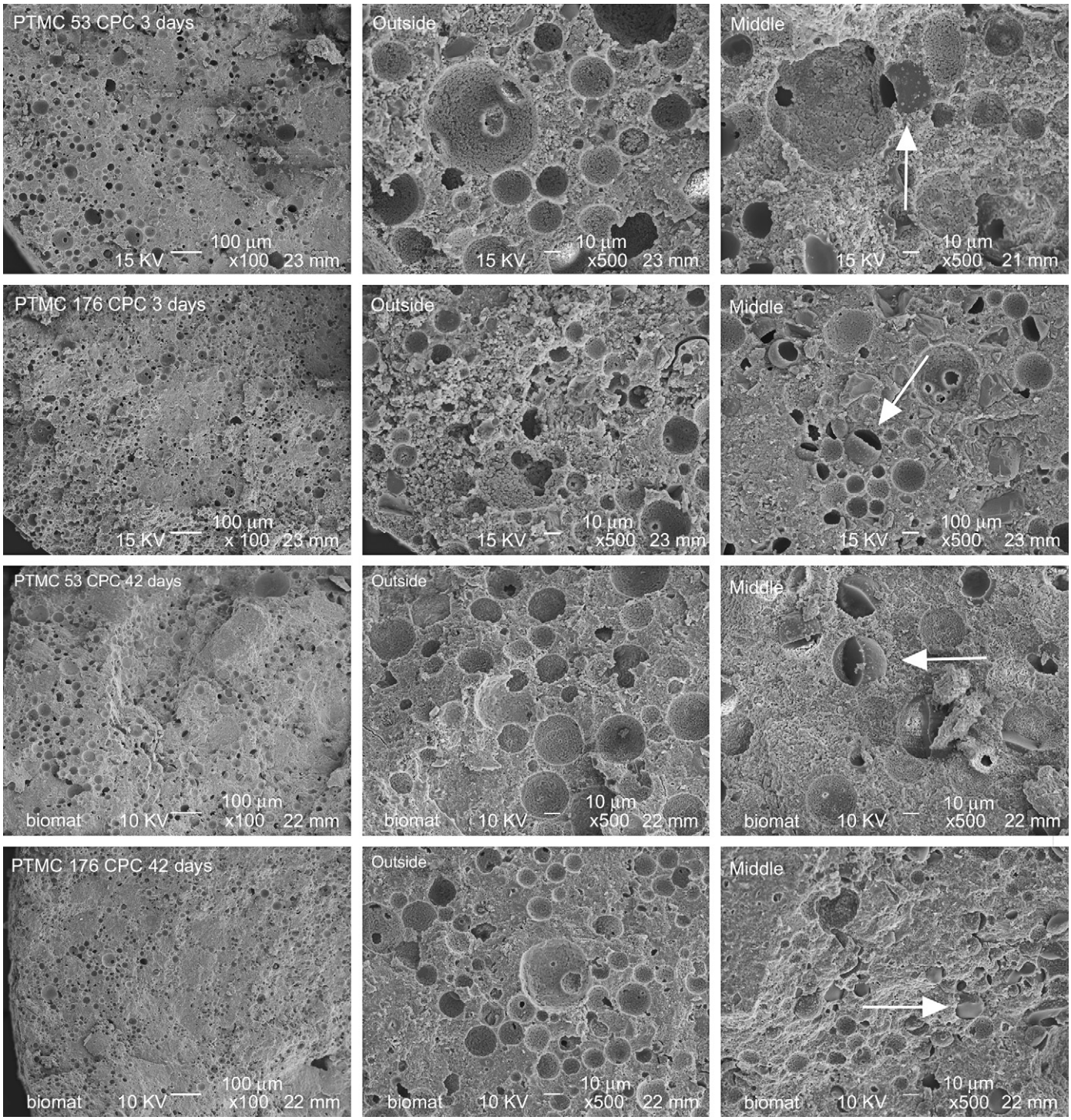

Fig. 10. SEM micrographs of the 12.5 wt% $PTMC_{53}$ CPC and $PTMC_{176}$ CPC samples after 3 and 42 days in lipase solution, arrows denote PTMC microspheres/shells (original magnification 100× and 500×).

PLGA microspheres [4] and gelatin microspheres [5] extra aqueous phase was present to improve the injectability of the composite (PLGA) or as a result of the preparation method (pre-swollen gelatin microspheres). Another parameter that influenced the setting of PTMC CPC is the large volume of microspheres of especially the 25 wt% PTMC CPC that hampers the entanglement of calcium phosphate crystals (setting process) [17]. Furthermore, even after the cement has set, imprints of the Gilmore needle were still visible as a result of plastic deformation of the composite [18].

For the degradation study PBS as well as a lipase solution were used. Though in PBS no degradation of the microspheres is expected, this study was necessary to compare the current results with microsphere CPC specimens in previous experiments

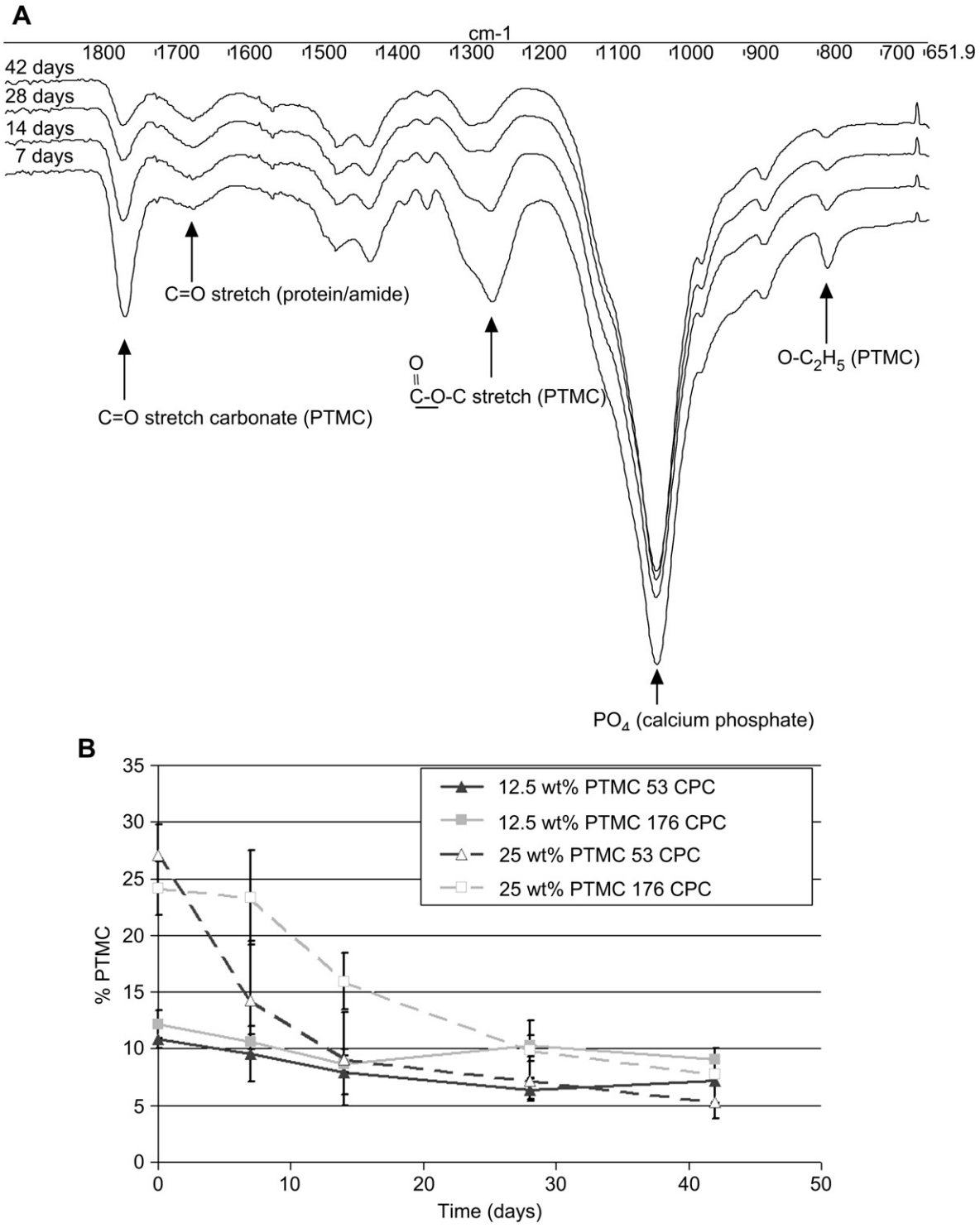

Fig. 11. A) IR spectra of the 25 wt% $PTMC_{53}$ CPC in lipase medium after $t = 7$, 14, 28 and 42 days; (B) weight% of PTMC in samples as measured by FTIR as a function of incubation time in lipase solution.

[4–6]. Comparable to *in vitro* studies with pure PTMC specimens [11], the lipase solution was used to determine whether microspheres within a calcium phosphate scaffold could degrade in the presence of a PTMC degrading enzyme. Although it has to be emphasized that in a bony environment the concentration of lipase will be much lower, implantation of solid PTMC scaffolds in the tibia and femur of rabbits [11] also resulted in a sustained surface erosion of the polymer indicating the presence of PTMC degrading enzymes.

Results of the pH assay for the degradation in PBS showed that a higher amount of incorporated PTMC microspheres results in a smaller pH decrease, indicating that the cement is the major source of acidic (degradation) products [4,19]. Furthermore, results of the PBS study showed that there was no sign

of PTMC degradation as an initial mass increase of 1.5–2.5% was measured, while the compression strength/E-modulus remained constant during the first 6 weeks of incubation. Nevertheless, after the first week the mass of the samples gradually decreased with time and also the compression strength decreased slightly after 12 weeks of incubation. As the same trend is observed with the CPC control, cement dissolution/degradation over time is the most plausible explanation. The initial mass increase was also observed in previous studies [5,6] and is caused by precipitation of salts from the PBS solution.

SEM pictures of the 25 wt% PTMC CPC specimens that were incubated in lipase solution showed an interconnected structure of macropores, which confirms that the microspheres have been degraded. At early time points ($t = 3$ days) this porosity was mostly present at the outer parts whereas at later time points, also at the inner radius the amount of microspheres was reduced. This result is comparable to that for the gelatin microsphere CPC in a previous experiment [6] and indicates a similar pattern with microspheres degrading from the outer to the inner part of the implants. Also results with IR showed a slow decrease in the wt% of PTMC within the composite, confirming a sustained degradation of the PTMC polymer. Both analyses showed that degradation of PTMC (microspheres) in the 12.5 wt% composites was much slower. This corresponds to studies with gelatin microspheres [5,6], and is caused by the low or non-existent interconnectivity of the microspheres that delays the penetration of lipase into the composite.

A striking observation in the IR spectra is that for the 25 wt% PTMC CPC, the $PTMC_{53}$ microspheres inside the cement degrade faster than the $PTMC_{176}$ microspheres, whereas the highest molecular weight PTMC degrades faster in separate degradation experiments [11]. As $PTMC_{176}$ microspheres were significantly smaller than the $PTMC_{53}$ microspheres, they also contained a relatively higher amount of hydrophilic PVA at the surface [20]. This may form a barrier for enzymatic degradation as the enzymes are more active at hydrophobic surfaces. The difference in size of the $PTMC_{53}$ and $PTMC_{176}$ microspheres was related to different parameters that were applied in their preparation.

The results from the mass assay do not corroborate with the IR and SEM results. If mass decrease would be in agreement with these results, the mass of the 25 wt% PTMC CPC should have decreased to 15–20% after 6 weeks. However, only an initial decrease in mass was observed followed by a slow increase in mass. The reason for this phenomenon is that within this system there are two processes occurring at the same time, i.e. degradation of PTMC microspheres and adsorption of organic components (lipase) from the medium. Next to the appearance of a typical protein/amide-peak in IR spectra [21], occasionally a layer of precipitate at the surface of the sample was observed in SEM and the cement itself turned from white to yellow (color of lipase medium) with time.

For both the 12.5 and 25 wt% PTMC CPC either in PBS or in lipase solution, the compression strength/E-modulus remained constant with time. While in PBS there is no PTMC degradation, the compression strength of the PTMC CPC is expected to be constant. However, in lipase solution the 25 wt% PTMC CPC should show a decrease in compression strength [4–6] as the polymer is slowly degrading. Comparing the compression strengths of samples exposed to lipase solution with that of samples in PBS, the 25 wt% PTMC CPC samples (but also the 12.5 wt% PTMC CPC) have a lower value from the beginning (3 days) in lipase and no gradual decrease. This is probably due to the fact that the PTMC microspheres degrade by surface erosion [11] thereby detaching themselves from the surrounding cement. As a consequence, the compression strength decreases immediately after the start of microsphere degradation. A slower cement conversion rate in lipase solution as can be suggested from Fig. 7 is also an explanation for a lower initial mechanical strength, though in both the media the cement was highly converted into apatite after 14 days.

Finally, the introduction of a rubber-like PTMC into a calcium phosphate cement for tissue engineering possibly can be used to improve the mechanical properties of the cement, i.e. overcome brittleness [22], as a higher strain-at-yield was obtained with an increasing percentage of PTMC. Also the toughness of the cement increased as composites did not fracture after reaching the yield strength but were kept together by the elongated microspheres. Similar mechanical characteristics are also observed using fiber-containing calcium phosphate cements [23,24]. Compared to these fiber-containing cements, microsphere/calcium phosphate cement composites are more easy to process with respect to injectability and polymer distribution and therefore can form an attractive alternative.

5. Conclusion

Calcium phosphate cements incorporated with well distributed PTMC microspheres were formulated and showed initial setting times of ±2–3 min and compression strengths of 15–24 MPa. Gradual degradation of the incorporated microspheres occurred from the outer to the inner part of the composite when they were incubated in lipase solution, but not in PBS. The incorporation of PTMC microspheres in CPC improved the toughness of the material, preventing it from fracturing into smaller pieces.

Acknowledgements

Scanning electron microscopy was performed at the Microscopic Imaging Centre (MIC) of the Nijmegen Centre for Molecular Life Sciences (NCMLS), The Netherlands. This work was supported by the Dutch Technology Foundation STW, grant # NGT 6205.

References

[1] LeGeros RZ. Properties of osteoconductive biomaterials: calcium phosphates. Clin Orthop Rel Res 2002;395:81–98.
[2] Ooms EM, Wolke JGC, van de Heuvel MT, Jeschke B, Jansen JA. Histological evaluation of the bone response to calcium phosphate cement implanted in cortical bone. Biomaterials 2003;24(6):989–1000.

[3] Ruhé PQ, Kroese-Deutman H-C, Wolke JGC, Spauwen PHM, Jansen JA. Bone inductive properties of rhBMP-2 loaded porous calcium phosphate cement implants in cranial defects in rabbits. Biomaterials 2004;25: 2123–32.

[4] Habraken WJEM, Wolke JGC, Mikos AG, Jansen JA. Injectable PLGA microsphere/calcium phosphate cements: physical properties and degradation characteristics. J Biomat Sci Polym Ed 2006;17(9):1057–74.

[5] Habraken WJEM, de Jonge LT, Wolke JGC, Yubao L, Mikos AG, Jansen JA. Introduction of gelatin microspheres into an injectable calcium phosphate cement. J Biomed Mater Res Part A 2008 Jan 11 [Epub ahead of print].

[6] Habraken WJEM, Wolke JGC, Mikos AG, Jansen JA. Porcine gelatin microsphere/calcium phosphate cement composites: in vitro degradation and drug release. J Biomed Mater Res Part B Appl Biomat, submitted for publication.

[7] Ruhé PQ, Boerman OC, Russel FG, Spauwen PH, Mikos AG, Jansen JA. Controlled release of rhBMP-2 loaded poly(D,L-lactic-*co*-glycolic acid)/ calcium phosphate cement composites in vivo. J Control Release 2005;106(1–2):162–71.

[8] Holland TA, Tabata Y, Mikos AG. Dual growth factor delivery from degradable oligo(poly(ethylene glycol) fumarate) hydrogel scaffolds for cartilage tissue engineering. J Control Release 2005;101(1–3): 111–25.

[9] Bigi A, Boanini E, Panzavolta S, Roveri N, Rubini K. Bonelike apatite growth on hydroxyapatite-gelatin sponges from simulated body fluid. J Biomed Mater Res Part A 2002;59:709–14.

[10] Albertsson A-C, Eklund M. Infuence of molecular structure on the degradation mechanism of degradable polymers: in vitro degradation of poly(trimethylene carbonate), poly(trimethylene carbonate-*co*-caprolactone) and poly(adipic anhydride). J Appl Polym Sci 1995;57:87–103.

[11] Zhang Z, Kuijer R, Bulstra SK, Grijpma DW, Feijen J. The in vivo and in vitro behavior of poly(trimethylene carbonate). Biomaterials 2006;27(9): 1741–8.

[12] Zhang Z, Zou S, Vansco GJ, Grijpma DW, Feijen J. Enzymatic surface erosion of poly(trimethylene carbonate) films studied by atomic force microscopy. Biomacromolecules 2005;6(6):3404–9.

[13] Zhang Z, Foks MA, Grijpma DW, Feijen J. PTMC and MPEG–PTMC microparticles for hydrophilic drug delivery. J Control Release 2005;101(1–3):392–4.

[14] Featherstone JDB, Pearson S, LeGeros RZ. An infrared method for quantification of carbonate in carbonated apatites. Caries Res 1984;18:63–6.

[15] Pêgo AP, Poot AA, Grijpma DW, Feijen J. Physical properties of high molecular weight 1,3-trimethylene carbonate and D,L-lactide copolymers. J Mater Sci Mater Med 2003;14(9):767–73.

[16] Khairoun I, Boltong MG, Driessens FCM, Planell JA. Effect of calcium carbonate on clinical compliance of apatitic calcium phosphate bone cement. J Biomed Mater Res Part A 1997;38:356–60.

[17] Liu C, Shen W, Yanfang G, Hu L. Mechanism of the hardening process for a hydroxyapatite cement. J Biomed Mater Res Part A 1997;35:75–80.

[18] Zhang Z, Grijpma DW, Feijen J. Triblock copolymers based on 1,3-trimethylene carbonate and lactide as biodegradable thermoplastic elastomers. Macromol Chem Phys 2004;205:867–75.

[19] Link DP, van den Dolder J, Wolke JG, Jansen JA. The cytocompatibility and early osteogenic characteristics of an injectable calcium phosphate cement. Tissue Eng 2007;13(3):493–500.

[20] Panyam J, Dali MM, Sahoo SK, Ma W, Chakravarthi SS, Amidon GL, et al. Polymer degradation and in vitro release of a model protein from poly(D,L-lactide-*co*-glycolide) nano- and microparticles. J Control Release 2003;92:173–87.

[21] Pouchert CJ, editor. The Aldrich library of infrared spectra. 3rd ed. 1981. p. 435.

[22] Habraken WJ, Wolke JG, Jansen JA. Ceramic composites as matrices and scaffolds for drug delivery in tissue engineering. Adv Drug Deliv Rev 2007;59(4–5):234–48.

[23] Buchanan F, Gallagher L, Jack V, Dunne N. Short-fibre reinforcement of calcium phosphate bone cement. Proc Inst Mech Eng 2007;221(2):203–11.

[24] Xu HH, Quinn JB. Calcium phosphate cement containing resorbable fibers for short-term reinforcement and macroporosity. Biomaterials 2002;23(1):193–202.